

TECHNICAL REPORT  
NATICK/TR-89/013

AD \_\_\_\_\_

# LOW SPEED AIR-FLOW CHARACTERIZATION OF MILITARY FABRICS

BY

LANDA HOKE  
R.A. SEGARS  
S. COHEN  
A. KING  
E. JOHNSON

OCTOBER 1988

FINAL REPORT  
NOVEMBER 1986 TO SEPTEMBER 1987

APPROVED FOR PUBLIC RELEASE;  
DISTRIBUTION UNLIMITED

UNITED STATES ARMY NATICK  
RESEARCH, DEVELOPMENT AND ENGINEERING CENTER  
NATICK, MASSACHUSETTS 01760-5000

SCIENCE AND ADVANCED TECHNOLOGY DIRECTORATE

### DISCLAIMERS

The findings contained in this report are not to be construed as an official Department of the Army position unless so designated by other authorized documents.

Citation of trade names in this report does not constitute an official endorsement or approval of the use of such items.

### DESTRUCTION NOTICE

#### For Classified Documents:

Follow the procedures in DoD 5200.22-M, Industrial Security Manual, Section II-19 or DoD 5200.1-R, Information Security Program Regulation, Chapter IX.

#### For Unclassified/Limited Distribution Documents:

Destroy by any method that prevents disclosure of contents or reconstruction of the document.

REPORT DOCUMENTATION PAGE				Form Approved OMB No. 0704-0188 Exp. Date: Jun 30, 1986	
1a. REPORT SECURITY CLASSIFICATION UNCLASSIFIED		1b. RESTRICTIVE MARKINGS			
2a. SECURITY CLASSIFICATION AUTHORITY		3. DISTRIBUTION / AVAILABILITY OF REPORT Approved for public release; Distribution unlimited.			
2b. DECLASSIFICATION / DOWNGRADING SCHEDULE					
4. PERFORMING ORGANIZATION REPORT NUMBER(S) NATICK/TR-89/013		5. MONITORING ORGANIZATION REPORT NUMBER(S)			
6a. NAME OF PERFORMING ORGANIZATION U.S. Army Natick RD&E Center Biochem Br, BioSD, SATD		6b. OFFICE SYMBOL (if applicable) STRNC-YMB	7a. NAME OF MONITORING ORGANIZATION		
6c. ADDRESS (City, State, and ZIP Code) Kansas St. Natick, MA 01760-5020		7b. ADDRESS (City, State, and ZIP Code)			
8a. NAME OF FUNDING / SPONSORING ORGANIZATION		8b. OFFICE SYMBOL (if applicable)	9. PROCUREMENT INSTRUMENT IDENTIFICATION NUMBER		
8c. ADDRESS (City, State, and ZIP Code)		10. SOURCE OF FUNDING NUMBERS			
		PROGRAM ELEMENT NO. 611102A	PROJECT NO. AH52	TASK NO. 01	WORK UNIT ACCESSION NO. DA311625
11. TITLE (Include Security Classification) (U) Low Speed Air-Flow Characterization of Military Fabrics					
12. PERSONAL AUTHOR(S) Hoke, Landa, Segars, R.A., Cohen, S., King, A. and Johnson, E.					
13a. TYPE OF REPORT Final		13b. TIME COVERED FROM Nov 86 TO Sep 87	14. DATE OF REPORT (Year, Month, Day) 88 October		15. PAGE COUNT 35
16. SUPPLEMENTARY NOTATION					
17. COSATI CODES			18. SUBJECT TERMS (Continue on reverse if necessary and identify by block number)		
FIELD	GROUP	SUB-GROUP	Fabrics	Air Flow	Fabric Structure
			Membranes	Polyester	Air Permeability
				Porosity	Military cloth
					Nylon
					Cotton
					Models
19. ABSTRACT (Continue on reverse if necessary and identify by block number)  Low speed air-flow studies have been conducted in order to characterize military cloth. Measurements were performed on the military cloth nylon/cotton (NYCO); in addition, cloth samples with specified pore size, open area and thickness were examined in order to develop criteria to characterize NYCO as well as other military fabrics. Data of air velocity through a cloth and corresponding pressure drop across the cloth were successfully modeled in two ways. The first was by application of a model based on air-flow through a single pore or orifice to the problem of air-flow through cloth samples which contain many pores. The second was by applying a model developed for air-flow through wire meshes or screens to air-flow through cloth.					
20. DISTRIBUTION / AVAILABILITY OF ABSTRACT <input checked="" type="checkbox"/> UNCLASSIFIED/UNLIMITED <input type="checkbox"/> SAME AS RPT. <input type="checkbox"/> DTIC USERS			21. ABSTRACT SECURITY CLASSIFICATION UNCLASSIFIED		
22a. NAME OF RESPONSIBLE INDIVIDUAL Landa Hoke		22b. TELEPHONE (Include Area Code) (508)651-4550		22c. OFFICE SYMBOL STRNC-YMB	



## PREFACE

This project on modeling air flow through military cloth was undertaken during the period November 1986 to September 1987. It was funded under Program Element No. 611102A, Project No. AH52, Task No. 01 and Work Unit Accession No. DA311625.

Thanks are due to John Halliday for his detailed and helpful comments and to Margaret Goode for supplying the NYCO photograph and for valuable advice. Gerald Silverman's constructive comments are appreciated. Marcia Lightbody's suggestions contributed to this report. Thanks are also due to Patricia Crawford and Marlene Jewer for their accuracy and speed in typing the manuscript and to Patricia Crawford for her patience and encouragement.



## TABLE OF CONTENTS

	<u>PAGE</u>
PREFACE	iii
LIST OF FIGURES	vi
LIST OF TABLES	vii
INTRODUCTION	1
INITIAL EXPERIMENTS	1
MATHEMATICAL MODELS TO CHARACTERIZE FABRICS	8
SUMMARY AND CONCLUSIONS	24
RECOMMENDATIONS FOR FUTURE WORK	24
REFERENCES	26
APPENDIX A - Raw Data for Air-Flow Measurements	27
APPENDIX B - List of Symbols Used	28
DISTRIBUTION LIST	29

## LIST OF FIGURES

<u>FIGURE</u>	<u>PAGE</u>
1. Air-flow Apparatus.	2
2. Comparison of measured and calculated air-flow rates for aluminum sheet 1 mm thick and hole of $0.137 \times 10^{-2}$ m diameter.	6
3. Discharge coefficient as a function of air-flow rate for aluminum sheet 0.1 mm thick with hole of $0.21 \times 10^{-2}$ m diameter.	6
4. Pressure drop across a cloth sample as a function of air-flow rate through the cloth.	10
5. Pressure drop across a cloth sample as a function of air-flow rate through the cloth. Comparison of 10 $\mu$ m pore size cloth with NYCO.	10
6. (A) 80 $\mu$ m Polyester Filter, Light Microscope (B) 67 $\mu$ m Polyester Filter, Light Microscope (C) 53 $\mu$ m Polyester Filter, Light Microscope (D) 43 $\mu$ m Polyester Filter, Light Microscope (E) 33 $\mu$ m Polyester Filter, Light Microscope (F) 21 $\mu$ m Polyester Filter, Scanning Electron Microscope (G) 10 $\mu$ m Polyester Filter, Scanning Electron Microscope (H) Nylon/Cotton (NYCO), Scanning Electron Microscope (taken at approximately 50X: all others, (A)-(G) taken at approximately 200X)	13
7. Single pore air-flow model.	17
8. Comparison of 10 micrometer and NYCO cloths.	17
9. Wire grid or screen mesh model.	22
10. Wire grid or screen mesh model. Comparison of 10 micrometer and NYCO cloths.	22

## LIST OF TABLES

<u>TABLE</u>		<u>PAGE</u>
1.	Comparison of Measured and Calculated Air-flow Rates	5
2.	Dependence of Discharge Coefficient C on Flow Rate	7
3.	Model Polyester Cloth Specifications	8
4.	Air-flow through 10 $\mu\text{m}$ Cloth	15
5.	Results for Least Squares Analysis for F(q)	18
6.	Some Suggested Expressions for K	20
7.	Resistance Coefficient for 10 $\mu\text{m}$ Cloth	21
8.	Least Squares Analysis on Screen Mesh Model	23



# LOW SPEED AIR-FLOW CHARACTERIZATION OF MILITARY FABRICS

## INTRODUCTION

The goal of the work reported here is to develop methods to characterize the structure of military cloth using air-flow data. The ultimate goal is to develop a model that incorporates this and other information into an overall scheme whereby military fabrics in current use can be more accurately evaluated and also to supply information that can be incorporated into guidelines for improvement of future fabrics.

There is a large volume of literature dealing with air-flow through orifices and screens, which reflects the considerable quantity of research in the area. Our present objective is to correlate this type of air-flow measurement with specific physical parameters of a fabric such as the open area, thread diameter or mesh opening for simple fabrics or an "effective" open area for other fabrics, such as nylon/cotton (NYCO).

## INITIAL EXPERIMENTS

A diagram of the air-flow apparatus used in these experiments is shown in Fig. 1. Features to note in this diagram are the upstream and downstream pressure taps,  $P_1$  and  $P_2$  respectively, and the position of the sample (an aluminum sheet with a hole drilled in it or a piece of cloth). House air was used in these experiments. All experiments were performed at room temperature ( $\approx 20^\circ\text{C}$ ,  $68^\circ\text{F}$ ) and ambient relative humidity.

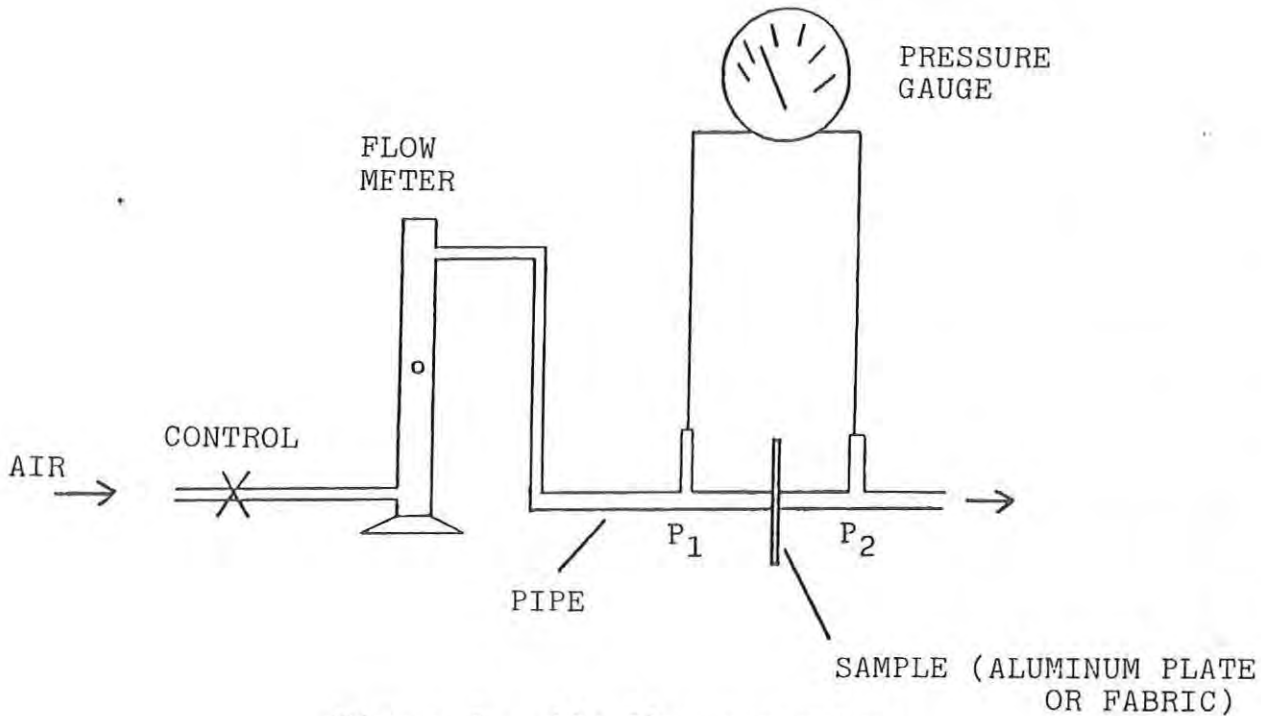


Figure 1. Air-flow apparatus.

In initial experiments, the test set-up and the data obtained from it were evaluated using a single pore (or orifice) air-flow model (1):

$$q = CYA \sqrt{(2g_c(p_1 - p_2))/(\rho[1 - \beta^4])}. \quad [1]$$

In equation [1], A is the cross-sectional area of the pore ( $m^2$ ),  $g_c$  is a constant ( $g_c$  equals one and is dimensionless in S.I. units),  $p_1$  is the pressure at the upstream tap ( $N/m^2$ ),  $p_2$  is the pressure at the downstream tap ( $N/m^2$ ),  $\rho$  is the air density at the upstream pressure tap ( $kg/m^3$ ),  $\beta$  is the ratio of the pore diameter to the pipe diameter (dimensionless), and  $q$  is the volume flow rate of air ( $m^3/s$ ) passing through the sample.

C is a dimensionless, numerical "coefficient of discharge" (1). Any effects on the air-flow due to stream contraction or friction are included in this factor. C depends upon the specific geometry of the apparatus and the velocity and viscosity of the air or fluid flowing through the system.

Y is an expansion factor (dimensionless), which accounts for a change in density of the air as it expands adiabatically (no heat flowing into or out of the system) in going from a pressure  $p_1$ , to a pressure  $p_2$ . Y is a function of the pore to pipe diameter ratio  $\beta$ , the downstream to upstream pressure ratio  $p_2/p_1$ , and the ratio of the specific heats  $c_p/c_v$  (1).

It is instructive to review in detail two examples of the initial work, which were preliminary to the study of cloth samples.

First Example: In the first experiment, the sample was an aluminum sheet 1 mm thick which contained a single circular hole (pore)  $0.137 \times 10^{-2}$  m diameter. For this experiment, the pipe diameter of the apparatus was  $2.4 \times 10^{-2}$  m. The measured quantities were  $q$  the air-flow rate through the hole and the pressure drop  $\delta p$  ( $p_1 - p_2$ ) due to the presence of the hole. The upstream pressure tap was situated approximately 5-1/2 pipe diameters away from the sample and the downstream pressure tap about two pipe diameters away from the sample.

In order to calculate air-flow rates  $q$  from equation [1], we used the following values:  $\beta$  for this example was 0.057 ( $=0.137/2.4$ ) and  $\beta^4$  is approximately  $10^{-5}$ . This is much less than one, so  $\beta^4$  was neglected. The air density,  $\rho$ , at the upstream pressure tap was assigned a value of  $1.205 \text{ kg/m}^3$ , which is the density of dry air at room temperature and

atmospheric pressure (2). In reference (1) some Y values for orifices are given. Values range from 0.92 to 1.00. For this preliminary calculation Y was assigned a value of 1.00. The cross-sectional area, A, of the pore was  $1.47 \times 10^{-6} \text{ m}^2$ .

This leaves C, the discharge coefficient, undetermined. C depends on several factors, one of which is the air-flow rate through the pore. In this first example the dependence of C on air-flow rate is neglected and C is treated as a constant. (In the second example, however, the dependence of C on air-flow rate is examined.)

In the first example, the C value associated with each q and  $\delta p$  data point was calculated using equation [1]. See Table 1. These C values appeared to have a random distribution and they have a mean of 0.82 with a standard deviation of 0.018. This mean C value can be used along with equation [1] to predict a flow rate for a given pressure drop. A good agreement was obtained between predicted and observed air-flow rates. This information is presented in Table 1 and shown graphically in Figure 2. Note that the air-flow was measured with a flow meter calibrated in mL/min and  $\delta p$  was measured with a pressure gauge calibrated in inches of water. The range of measurements here was limited by the pressure gauge available to about 13.5 inches of water.

The pressure drop across the apparatus alone (no sample present) between  $P_1$  and  $P_2$  (see Fig. 1) is a function of air flow rate. For the data given in this report, these pressure drops are very small compared to the pressure drops due to the samples and are neglected.

TABLE 1. Comparison of Measured and Calculated Air-flow Rates  
(aluminum sheet 1 mm thick with hole of  $0.137 \times 10^{-2}$  m  
diameter)

$\delta p$ (pascals $\times 10^2$ )	$q$ ( $m^3/s \times 10^{-5}$ ) Measured	C Calculated Using equation 1	$q$ ( $m^3/s \times 10^{-5}$ ) Predicted Using C=0.82 and equation 1
1.4	1.92	0.85	1.8
1.5	1.92	0.82	1.9
5.58	3.54	0.79	3.66
5.68	3.54	0.78	3.69
11.2	5.19	0.82	5.19
11.6	5.19	0.80	5.28
18.7	6.84	0.83	6.70
19.2	6.84	0.82	6.79
29.63	8.48	0.82	8.44
30.00	8.48	0.82	8.49
32.69	8.98	0.83	8.86
33.62	8.89	0.81	8.99

The conclusion from this first example is that for the air-flow range  $1.92 \times 10^{-5}$  to  $8.98 \times 10^{-5} m^3/s$  and for the experimental conditions described above, treating C as a constant with respect to air-flow rate was a good approximation.

Second Example: For contrast, however, in the second example, when a larger range of air-flow values was examined,  $4.38 \times 10^{-5}$  to  $14.2 \times 10^{-5} m^3/s$ , the dependence of C on flow rate was evident. To achieve the higher flow rates, a different sample was required. The sample was again an aluminum sheet, but this time the hole diameter was larger ( $0.21 \times$

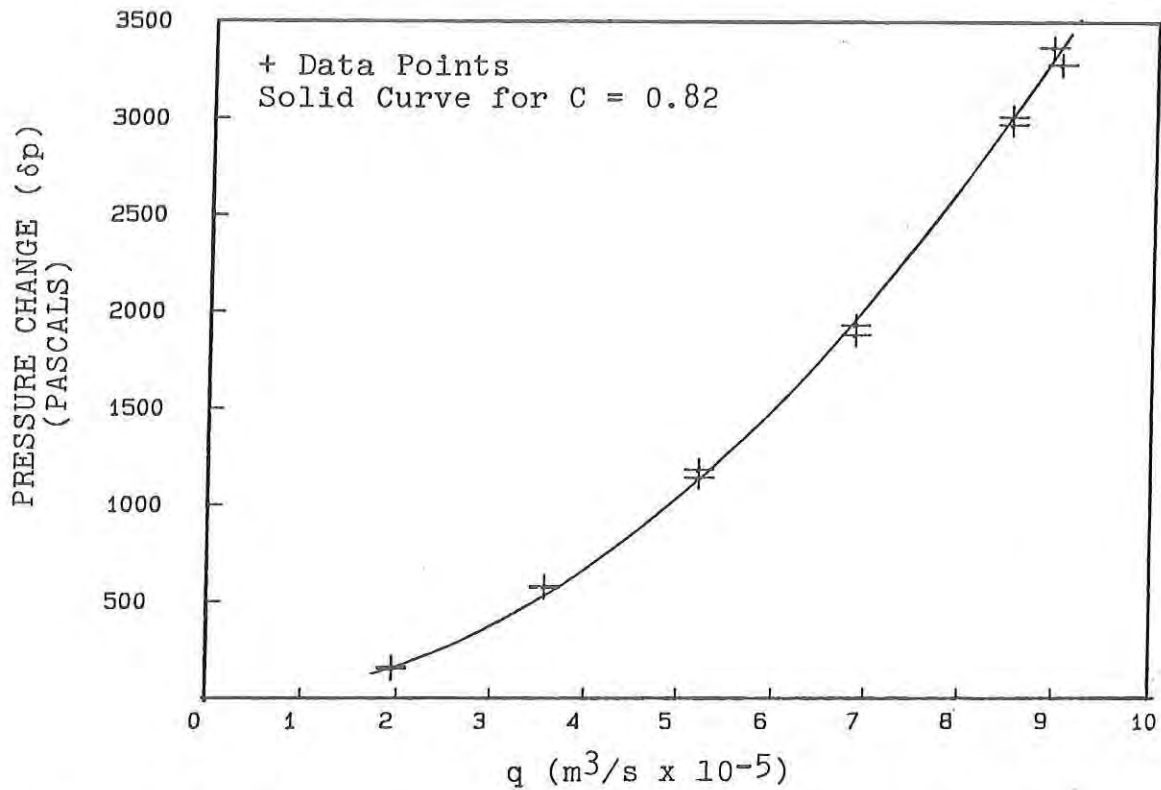


Figure 2. Comparison of measured and calculated air-flow rates for aluminum sheet 1 mm thick with hole of 0.137 x 10<sup>-2</sup> m diameter.

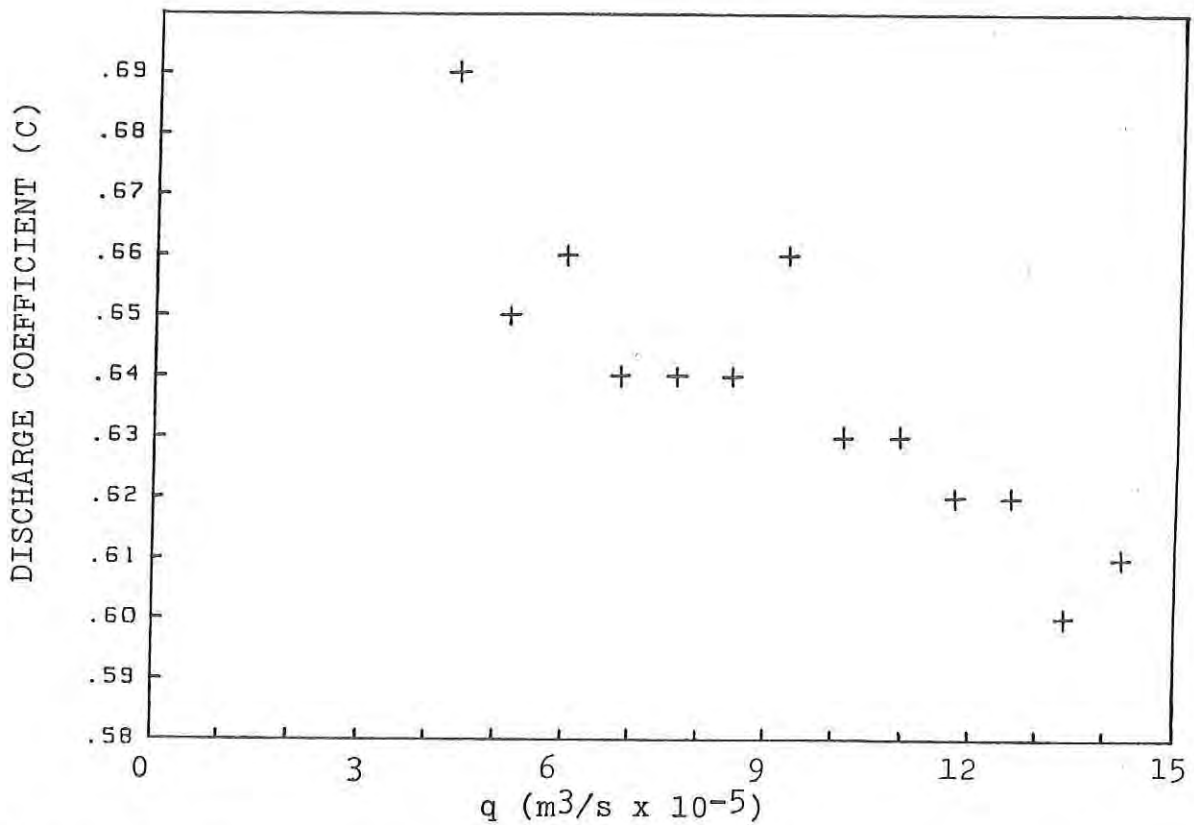


Figure 3. Discharge coefficient as a function of air-flow rate for aluminum sheet 0.1 mm thick with hole of 0.21 x 10<sup>-2</sup> m diameter.

$10^{-2}$  m) and the sheet was thinner ( $0.1 \times 10^{-3}$  m). Using the same approximations as for the first example, equation [1] can be written for this case

$$q = C(4.46 \text{ m}^{7/2} \text{ kg}^{-1/2} \times 10^{-6})\sqrt{\delta p}, \quad [2]$$

where  $\delta p = p_1 - p_2$  is the pressure drop across the sample in pascals.

For this example, there were 13 data points ( $q, \delta p$  pairs). Using equation [2] and calculating values of C for each  $\{q, \delta p\}$  pair shows the flow rate dependence of C. These results are given in Table 2 and Figure 3.

TABLE 2. Dependence of Discharge Coefficient C on Flow Rate (aluminum sheet 0.1 mm thick with hole of  $0.21 \times 10^{-2}$  m diameter)

$\delta p$ (pascals $\times 10^2$ )	$q$ ( $\text{m}^3/\text{s} \times 10^{-5}$ )	C (calculated from equation 2)
2	4.37	0.69
3.2	5.18	0.65
4.2	6.00	0.66
5.7	6.82	0.64
7.2	7.64	0.64
8.7	8.47	0.64
10	9.29	0.66
13	10.13	0.63
15	10.95	0.63
18	11.77	0.62
21	12.60	0.62
25	13.42	0.60
27.6	14.24	0.61

It can be seen that the discharge coefficient  $C$  decreases as the flow rate  $q$  increases. (The pressure values cover a smaller range in this example (Table 2) than they did in the previous example (Table 1).) This dependence of  $C$  on air-flow rate, which is evident in Table 2 and which produces a deviation in the "expected" square root dependence of  $\delta p$  on  $q$ , must be taken into account if modeling efforts are to be successful.

#### MATHEMATICAL MODELS TO CHARACTERIZE FABRICS

The ultimate objective is to understand air-flow through military cloth. Experiments and analyses similar to the examples shown above provided a means to check the  $\delta p$  and corresponding  $q$  values obtained with the apparatus and in the interpretation of the data. The next step was to examine cloth samples. These samples include "model" cloths (with specified mesh openings, open areas, and mesh thickness) from SPECTRUM and the military cloth NYCO (50% cotton and 50% nylon, 7 oz/yd<sup>2</sup>, twill weave, Quarpel coated). The manufacturer's specifications (3) for the model cloths are given in Table 3. The mesh number is also indicated. In addition, thread diameters are included (4). Note that no tolerances on the specifications are reported in the SPECTRUM catalogue.

TABLE 3. Model Polyester Cloth Specifications (3)

Mesh Opening ( $\mu\text{m}$ )	Open Area (%)	Thread Diameter ( $\mu\text{m}$ )	Mesh Thickness ( $\mu\text{m}$ )	Mesh Number
*10	3	?	70	?
*21	15	33	70	M470
33	25	42	65	M340
43	29	38	70	M315
53	34	40	70	M270
67	41	38	70	M240
80	38	48	90	M200

\* Flattened by Spectrum

Air-flow measurements were conducted using these model cloths and NYCO. Plots of pressure drop across the cloth versus air-flow rate through the cloth are shown in Figs. 4 and 5. It is conventional in fabric studies to normalize the volume flow rate  $q$  ( $\text{m}^3/\text{s}$ ) by dividing by the cross-sectional area of the pipe (diameter of  $9.34 \times 10^{-3} \text{m}$  and area of  $6.85 \times 10^{-5} \text{m}^2$ ). The normalized volume flow rate will be denoted by  $Q$  ( $\text{m}^3/\text{s}/\text{m}^2$ ). Figure 5 shows that the same shape of  $\delta p$  versus  $Q$  plot is obtained for NYCO as for the polyester filters. A table listing these air-flow data is given in Appendix A. The average linear upstream velocities for these fabric experiments ranged from approximately 0.6 mph to 6 mph.

Light microscope or scanning electron microscope (SEM) photographs were taken of the polyester filters and NYCO. For the light microscopy, the polyester filter was placed on a clear glass microscope slide, which was put onto the stage of a Zeiss Ultraphot microscope equipped with a Nomarski condenser and a Neofluor 16X objective. Transmitted light micrographs were taken using Polaroid 55 P/N film. A scale was also photographed to determine the approximate magnification. Light areas, which appear on some of the fibers in these photographs, indicate where the transmitted light travelled through the fiber and reached the camera. These spots are not indications of open areas. Note that the polyester filters appear white when viewed in daylight. For the scanning electron microscopy, a piece of polyester filter approximately  $1 \text{ cm}^2$  was placed onto an aluminum stub using double-sided sticky tape and then sputter coated with a conductive layer of gold palladium. Then the sample was examined in a Hitachi 600-2

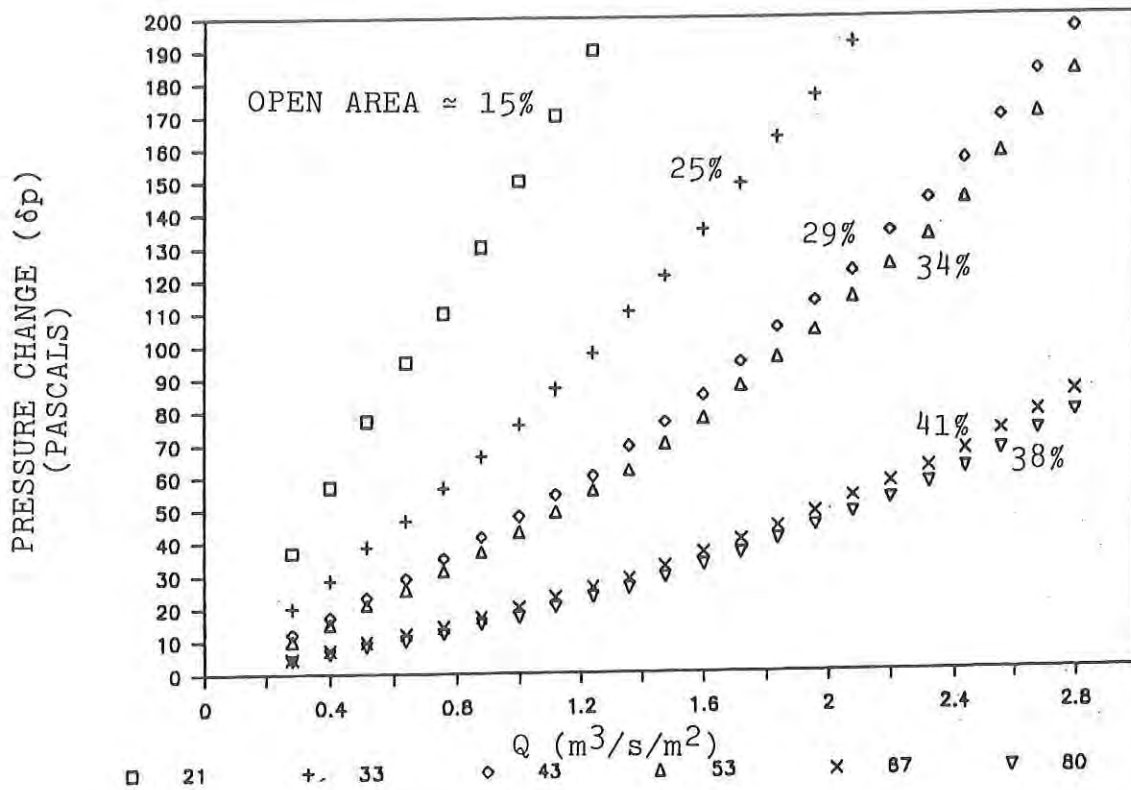


Figure 4. Pressure drop across a cloth sample as a function of air-flow rate through the cloth.

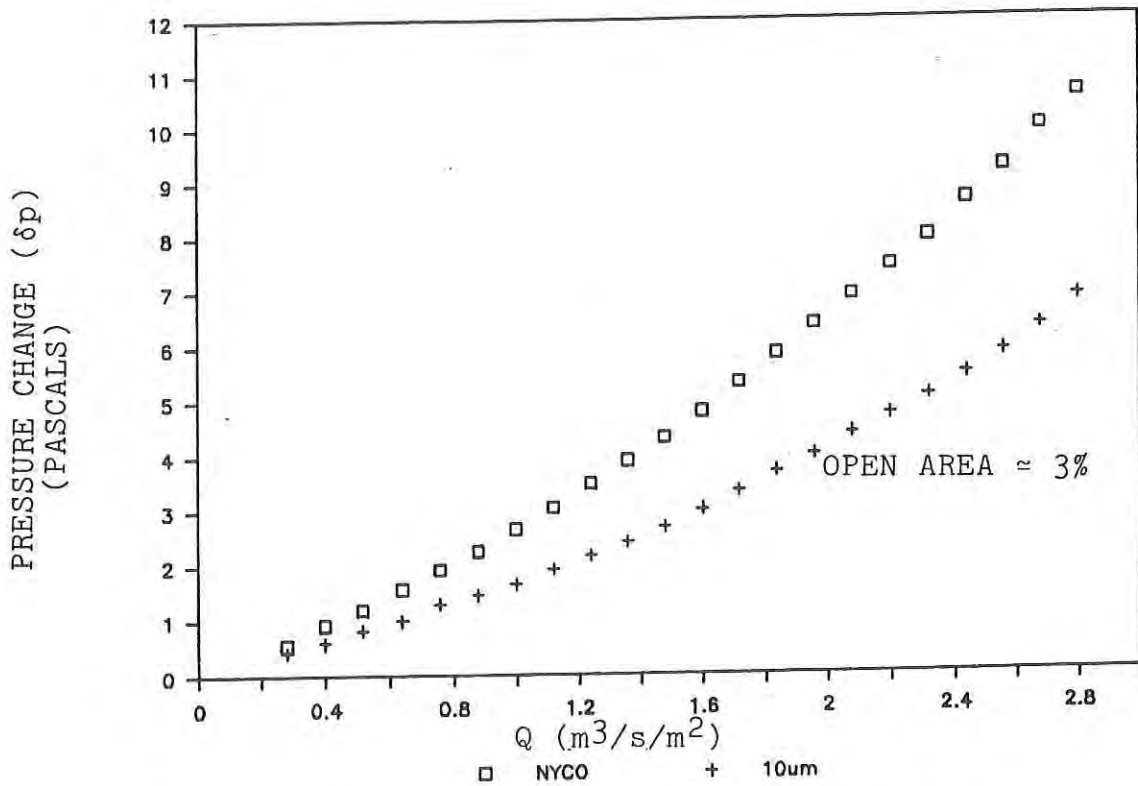


Figure 5. Pressure drop across a cloth sample as a function of air-flow rate through the cloth. Comparison of 10µm pore size with NYCO.

scanning electron microscope. Photographs were taken with Polaroid 55 P/N film. The light and SEM photographs are shown in Fig. 6.

An indication of the relative pore sizes, fiber diameters and open areas of the polyester filters is readily apparent in Fig. 6. For the NYCO fabric, the SEM photograph in this figure shows the yarns, the fibers, the weave and the surface structure. Pores cannot be seen. However, if a piece of NYCO is placed in front of a white light source, pinpoints of transmitted light are apparent at no magnification. These are indications of the largest pores and would be the major route for forced air-flow thorough this fabric.

Single Pore Model: The question at this point is how to model the data. Equation [1] pertains to a single hole or pore, but might be used as a starting point to develop a mathematical model for a sample with many pores such as cloth. The basic form of equation [1] is

$$q = F(q)\sqrt{2(\delta p)/\rho}. \quad [3]$$

In equation [3],  $F(q)$  is some unknown function of air-flow rate, which must be determined. Factors influencing the behavior of  $F(q)$  could be the discharge coefficient  $C$ , the percent open area of the sample, any interference effects due to the presence of multiple holes, the value of  $Y$  and any air density effects not properly accounted for in the estimated value of  $\rho(1.205 \text{ kg/m}^3)$ . Equation [3] can be rewritten in a form

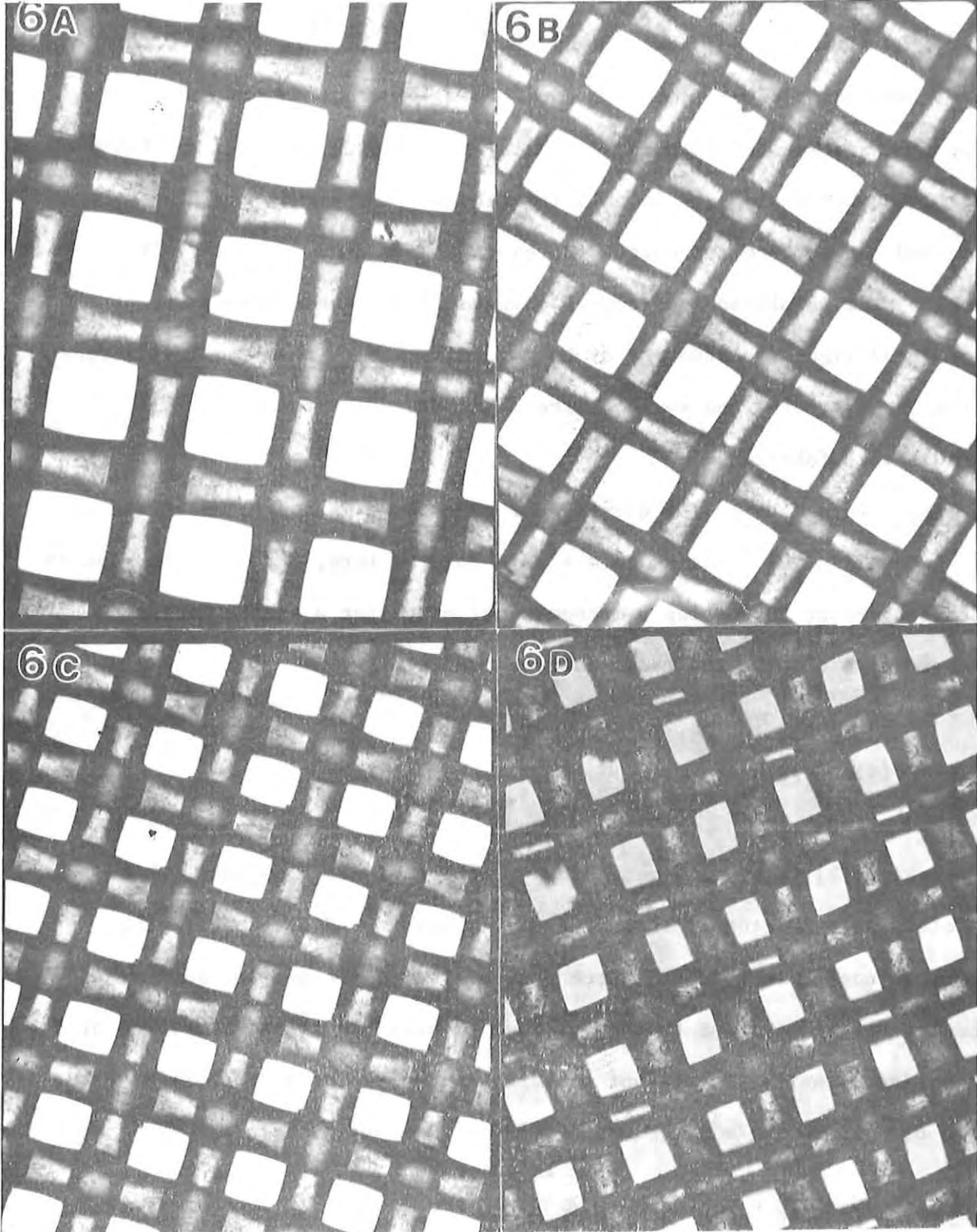


Figure 6A. 80  $\mu\text{m}$  Polyester Filter, Light Microscope.  
Figure 6B. 67  $\mu\text{m}$  Polyester Filter, Light Microscope.  
Figure 6C. 53  $\mu\text{m}$  Polyester Filter, Light Microscope.  
Figure 6D. 43  $\mu\text{m}$  Polyester Filter, Light Microscope.

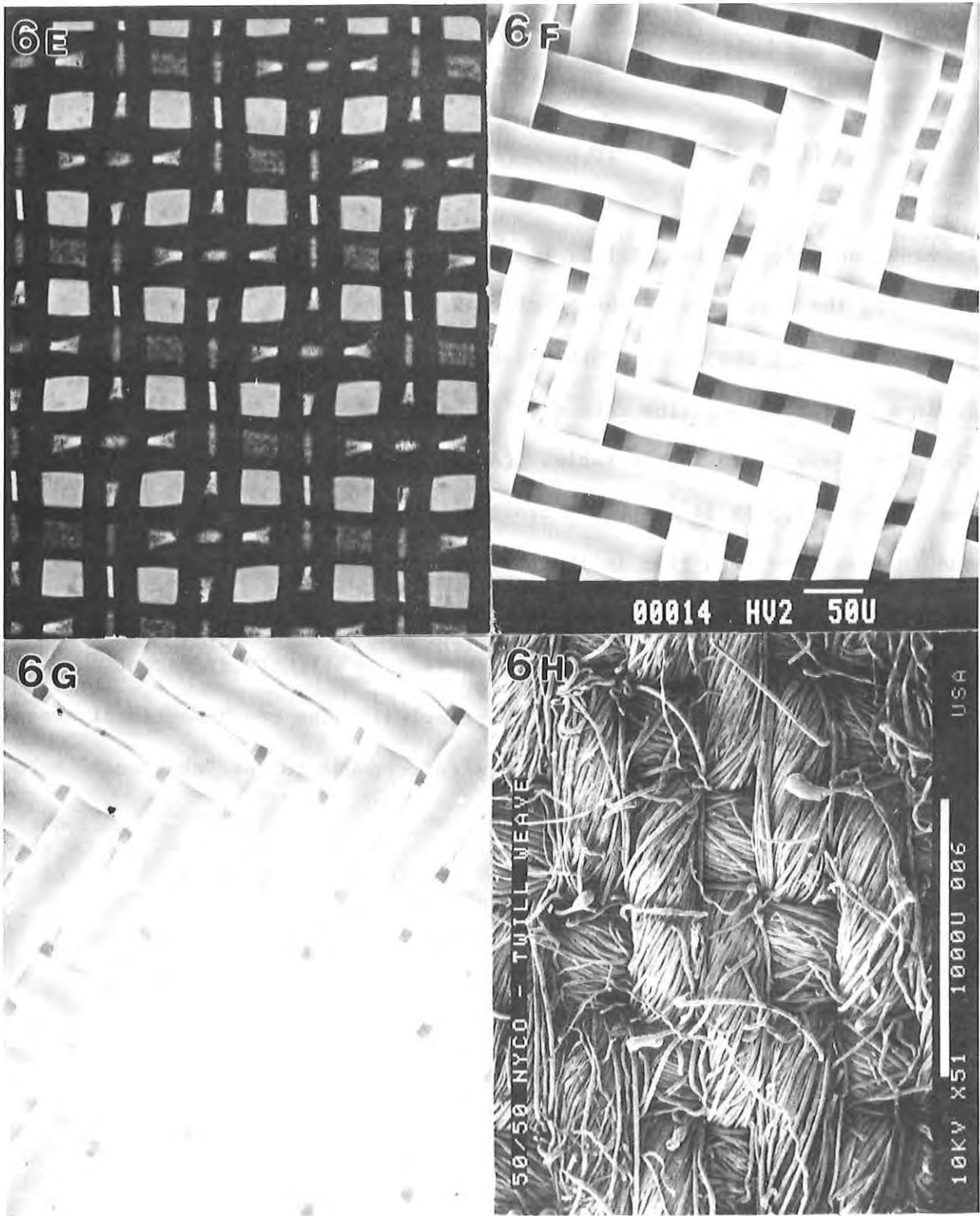


Figure 6E. 33  $\mu\text{m}$  Polyester Filters, Light Microscope.

Figure 6F. 21  $\mu\text{m}$  Polyester Filter, Scanning Electron Microscope.

Figure 6G. 10  $\mu\text{m}$  Polyester Filter, Scanning Electron Microscope.

Figure 6H. Nylon/Cotton (NYCO), Scanning Electron Microscope (taken at approximately 50X: all others. A-G taken at approximately 200X).

convenient to use directly with the cloth data (with units of  $m^3/s$  for  $q$  and pascals for  $\delta p$ ):

$$q = F(q)[1.29 m^{3/2} kg^{-1/2}] \sqrt{\delta p}. \quad [4]$$

In equation [4], the factor 1.29 is  $\sqrt{2/\rho}$ .  $F(q)$  contains information regarding the open area of the fabric and has units of  $m^2$ . The air-flow measurements for the  $10 \mu m$  cloth are typical of the data and are shown in Table 4. Both volume flow rate  $q$  ( $m^3/s$ ) and normalized volume flow rate  $Q(m^3/s/m^2)$  are given in the table. (Again note that the diameter of the pipe was  $9.34 \times 10^{-3} m$  with a cross-sectional area of  $6.85 \times 10^{-5} m^2$  and is a smaller area than in the previous two initial experiments. The upstream and downstream pressure taps were each situated approximately 2-1/2 pipe diameters from the sample. This is a slightly different configuration than in the two initial examples.) The cross-sectional area of the pipe in these fabric experiments corresponds to the "challenge" area in aerosol studies.

TABLE 4. Air-flow through 10  $\mu\text{m}$  Cloth

$\delta p$ (pascals)	$q$ ( $\text{m}^3/\text{s} \times 10^{-5}$ )	$Q$ ( $\text{m}^3/\text{m}^2/\text{s}$ )	$F(q)$ [ $\text{m}^2 \times 10^{-7}$ ]
430	1.92	0.280	7.18
600	2.74	0.400	8.67
820	3.54	0.517	9.58
1000	4.38	0.639	10.7
1300	5.19	0.758	11.2
1460	6.01	0.877	12.2
1660	6.84	0.998	13.0
1930	7.66	1.12	13.5
2180	8.48	1.24	14.1
2430	9.30	1.36	14.6
2690	10.13	1.48	15.1
3010	10.95	1.60	15.5
3350	11.77	1.72	15.8
3700	12.60	1.84	16.0
3990	13.42	1.96	16.5
4390	14.24	2.08	16.7
4720	15.06	2.20	17.0
5050	15.89	2.32	17.3
5450	16.71	2.44	17.5
5850	17.53	2.56	17.8
6320	18.35	2.68	17.9
6850	19.18	2.80	18.0

These data can be compared to that presented in Table 2 for air-flow through a single hole. It is instructive to examine the data for any deviations from the "expected" behavior of the flow rate dependence on the square root of the pressure drop as evidenced by the fact that  $F(q)$  is not a constant, but is a function of air flow rate.  $F(q)$  in Table 4 has a correspondence to the discharge coefficient  $C$  in Table 2. In this range of air-flow rates the data for a single hole show that as  $q$  increases,  $C$  decreases. For a sample with many small pores (e.g., cloth) the data show that in this flow range, as  $q$  increases,  $F(q)$  increases also. Some factors that are different with respect to the data in Table 2 versus the data in

Table 4 are a dramatic difference in hole size, a change in the frictional effects, and the possibility of interference effects due to the presence of multiple holes.

If a mathematical expression for  $F(q)$  could be determined based on the data, then it would be possible to predict the pressure drop across the cloth for a given air-flow rate through the cloth. Plots were constructed for  $F(q)$  versus  $q$  for our data. See the "data" points in Figs. 7 and 8. All the cloth samples as well as the NYCO displayed a similar shape. After several unsuccessful attempts to mathematically fit the data, an exponential function was examined:

$$F(q) = c - a \text{EXP}(-bq). \quad [5]$$

In equation [5]  $a$ ,  $b$ , and  $c$  are three parameters to be determined by statistical analysis. Equation [5] was used along with experimental  $q$  data and  $F(q)$  values ( $F(q)$  was determined as for the 10 micrometer cloth as shown in Table 4 using observed  $q$  and  $\delta p$  values along with equation [4]) to determine if the exponential function could explain the air-flow data. The three parameters ( $a$ ,  $b$ ,  $c$ ), which were determined for each cloth sample by least squares analyses, are given in Table 5.

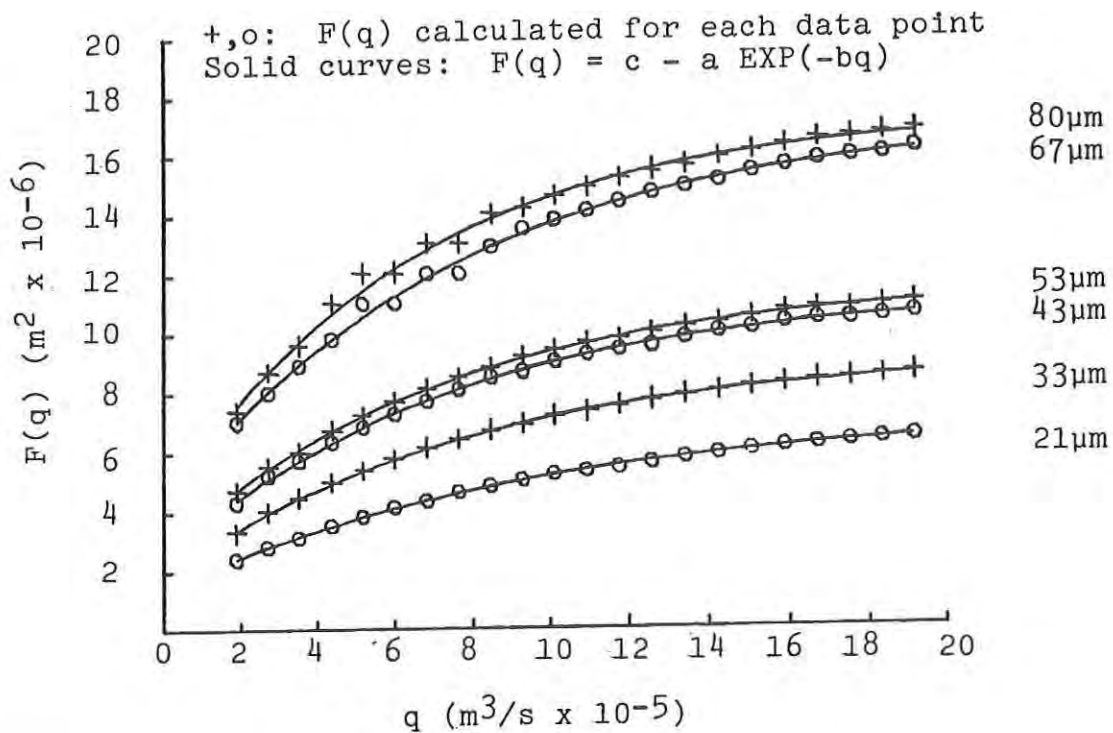


Figure 7. Single pore air-flow model.

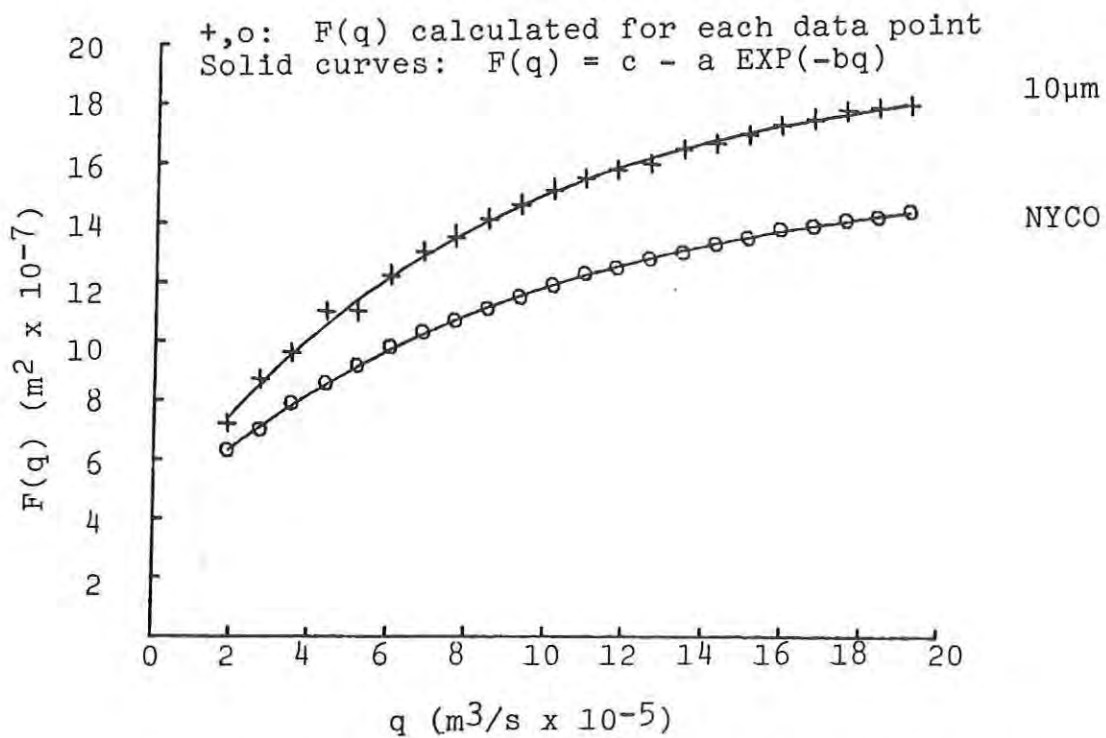


Figure 8. Comparison of 10 micrometer and NYCO cloths.

TABLE 5. Results of Least Squares Analyses for  $F(q)$

Cloth	(% Open Area)	$a$ ( $m^2 \times 10^{-4}$ )	$b$ ( $s/m^3 \times 10^4$ )	$c$ ( $m^2 \times 10^{-4}$ )
NYCO		0.0117	1.08	0.0158
10 $\mu m$	( 3%)	0.0152	1.24	0.0194
21 $\mu m$	(15%)	0.0590	1.03	0.0725
33 $\mu m$	(25%)	0.0746	1.25	0.0924
43 $\mu m$	(29%)	0.0895	1.33	0.113
53 $\mu m$	(34%)	0.0902	1.36	0.116
67 $\mu m$	(41%)	0.131	1.31	0.172
80 $\mu m$	(38%)	0.132	1.57	0.173

Using the parameter values from Table 5 an equation can be written for each cloth sample. For example, for NYCO

$$F(q) = 0.0158 \times 10^{-4} - 0.0117 \times 10^{-4} \text{EXP}(-1.08 \times 10^4 q). \quad [6]$$

Equations such as this one were plotted for the cloth samples and are shown as the solid curves in Figs. 7 and 8. These fitted curves have an excellent correspondence with the data. (Equations with other  $q$  dependences did not fit the data as well.) Table 5 shows that as the polyester filter's pore size and open area increase, the parameters  $a$  and  $c$  also, in general, increase. A next possible step in this type of analysis would be to mathematically correlate the parameters ( $a$ ,  $b$ ,  $c$ ) with cloth characteristics as given in Table 3 (mesh opening, open area, mesh thickness, thread diameter).

The success of these analyses suggests an air-flow equation for a cloth sample (based on the single pore model) for these flow conditions (experimental set-up and flow range)

$$q = [c-a \text{ EXP}(-bq)]\sqrt{2(\delta p)/\rho}. \quad [7]$$

Screen Mesh Model: In addition to the single pore air-flow model (equation [1]), an air-flow model used in the study of fluid flow through wire grids or screens was examined. This model has the same basic  $\delta p$  dependence on  $q$  as the single pore model but is expressed somewhat differently:

$$\delta p = (K\rho w^2)/2. \quad [8]$$

In equation [8],  $\delta p$  is the pressure drop across the sample (pascals),  $K$  is the resistance coefficient (dimensionless),  $\rho$  is the air density ( $\text{kg/m}^3$ ), and  $w$  (m/s) is the average upstream incident air velocity normal to the sample.  $w$  is equal to  $q(\text{m}^3/\text{s})$  divided by the cross-sectional area of the pipe ( $6.85 \times 10^{-5} \text{ m}^2$ ).

The resistance coefficient  $K$  is of particular interest because it has been explicitly associated with screen geometry in the literature. It is a function of several parameters:

$$K = K(\beta_1, R, M). \quad [9]$$

In equation [9],  $\beta_1$  is the porosity (ratio of open area to total area),  $R$  is the Reynold's number, and  $M$  is the Mach number.

TABLE 6. Some Suggested Expressions for K

Expression	Originator of Expression
1. $K = cs/(1-s)^2$	Weighardt and Others, in McCarthy <sup>5</sup>
2. $K = [(1-\beta_1)/\beta_1]^2$	Elder, in Turner <sup>6</sup>
3. $K = [C_2 (1 - \beta_1^2)]/\beta_1^2$	Annand, in Turner <sup>6</sup>
4. $K = K_0 + 88(1 - \beta_1)/R$	Davis, in Elder <sup>7</sup>

Examples of expressions for K are shown in Table 6. In this table  $s$  is the fraction of solid area of the sample  $(1 - \beta_1)$  and  $c$  and  $C_2$  are functions of the Reynold's number.  $K_0$  is a constant related to the screen geometry.

The data were analyzed based on the idea suggested by expression 4 in Table 6. Since the Reynold's number is directly proportional to the linear velocity  $w$ , this expression implies that K is inversely proportional to  $w$ . Therefore, if a plot is constructed of K versus  $1/w$ , a straight line should result. Values of K for the polyester filters and NYCO were determined from equation [8] using measured  $\delta p$  values, calculated  $w$  values and the density of air as  $1.205 \text{ kg/m}^3$ . An example showing the calculated K and corresponding  $w$  and  $1/w$  values for the  $10 \mu\text{m}$  cloth is given in Table 7. Plots of these data and the other cloth data are shown in Figs. 9 and 10. Least squares analyses were performed and the best fit straight lines are shown along with the data points in these figures. The squares of the correlation coefficients are given in Table 8 and they are very close to 1 for all cases. Results from statistical analyses for the slopes are also

given in this table. The slope is explicitly related to the open area  $\beta_1$  and the wire (or thread) diameter  $d$  (since  $R \propto d$ ) in expression 4. Note that the slope varies inversely with the open area  $\beta_1$  (or directly with the solid area  $(1-\beta_1)$ ). This feature can be seen in the calculated results for the cloth data in Table 8. Further additional attempts to achieve an exact correspondence between the cloth data and expression 4 were unsuccessful.

The assumption that  $K$  is directly proportional to  $w^{-1}$  produced a good fit to the data. However, the implication of this assumption is that  $\delta p$  becomes a linear function of  $w$  (see equation [8]).  $\delta p$ , though, is not exactly a linear function of  $w$  (or  $Q$ ) as can be seen in the plots presented in Figs. 4 and 5. Therefore, in order to obtain an even better fit to the data, it is desirable to examine other expressions for  $K$ .

TABLE 7. Resistance Coefficients for 10  $\mu\text{m}$  Cloth

$w$ (m/s)	$1/w$ (s/m)	$K \times 10^3$
0.280	3.57	7.78
0.400	2.50	5.39
0.517	1.93	4.44
0.639	1.56	3.66
0.758	1.32	3.14
0.877	1.14	2.73
0.998	1.00	2.40
1.12	0.893	2.22
1.24	0.806	2.05
1.36	0.735	1.90
1.48	0.676	1.77
1.60	0.625	1.69
1.72	0.581	1.63
1.84	0.543	1.57
1.96	0.510	1.50
2.08	0.481	1.46
2.20	0.455	1.40
2.32	0.431	1.35
2.44	0.410	1.32
2.56	0.391	1.29
2.68	0.373	1.27
2.80	0.357	1.26

o,x: K calculated for each data point  
 Solid curves: Least squares analyses

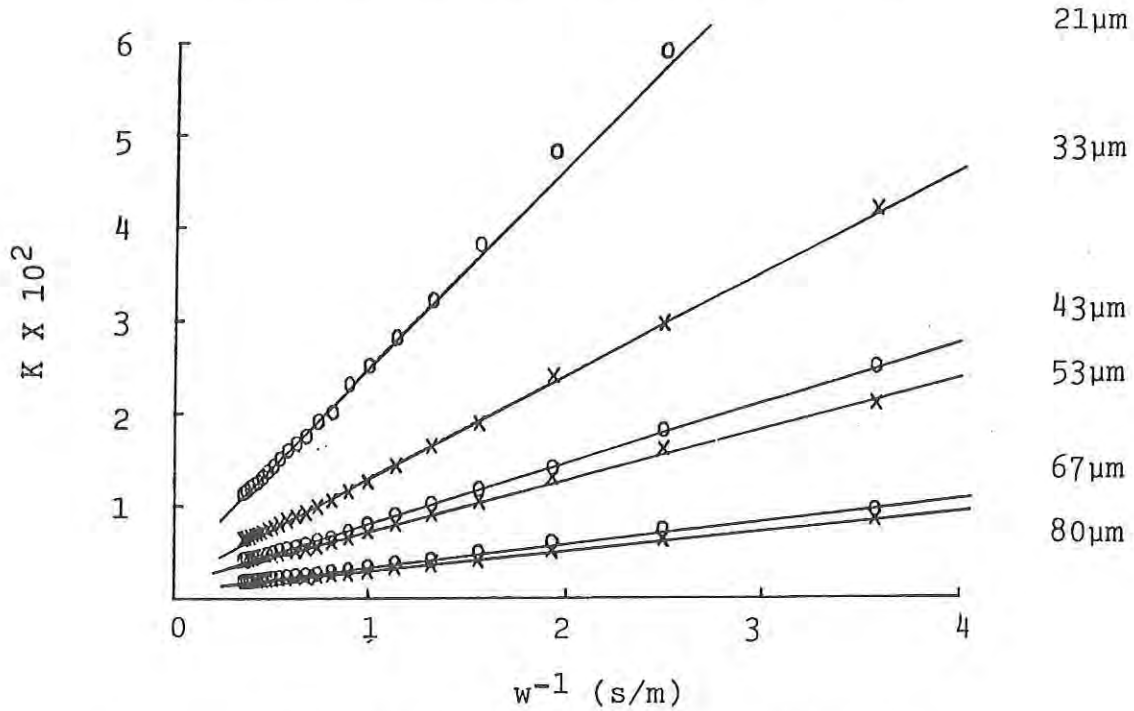


Figure 9. Wire grid or screen mesh model.

o,x: K calculated for each data point  
 Solid curves: Least squares analyses

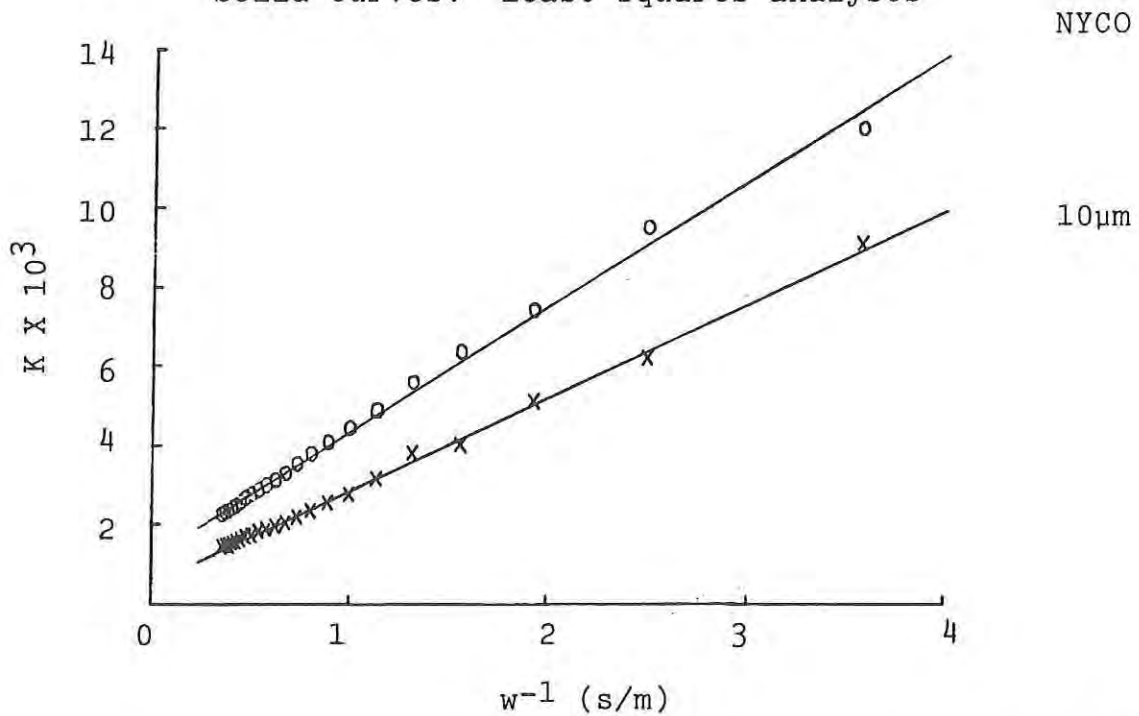


Figure 10. Wire grid or screen mesh model. Comparison of 10 micrometer and NYCO cloths.

TABLE 8. Least Squares Analyses on Screen Mesh Model

Cloth	(% Open Area)	Slope (m/s)	$r^2$
NYCO	?	3170	0.996
10 $\mu\text{m}$	( 3%)	2350	0.997
21 $\mu\text{m}$	(15%)	216	0.997
33 $\mu\text{m}$	(25%)	111	0.999
43 $\mu\text{m}$	(29%)	65.3	0.999
53 $\mu\text{m}$	(34%)	55.3	0.997
67 $\mu\text{m}$	(41%)	24.9	0.997
80 $\mu\text{m}$	(38%)	21.5	0.999

Recently, Ishizuka (8) suggested an expression in which K deviates somewhat from linearity

$$K = 28 \left[ \frac{R\beta_1^2}{(1-\beta_1)} \right]^{-0.95} \quad 0 < R < 100 \quad [10]$$

His work concerned natural air convection as related to designing electronic equipment casings. The Reynold's number can be defined

$$R = \frac{wd\rho}{\eta} \quad [11]$$

In equation [11] d is the thread diameter (m),  $\rho$  is the air density ( $\text{kg/m}^3$ ) and  $\eta$  is the viscosity ( $\text{kg/m-s}$ ). For the polyester filter data presented here the Reynold's numbers were below 10 so that equation [10] is appropriate. Initial calculations suggest that this equation corresponds well with the fabric data. However, some adjustments may be required.

## SUMMARY AND CONCLUSIONS

Methods to characterize military cloth with respect to low speed air-flow measurements have been examined. An air-flow apparatus that gives reproducible results has been constructed and data collected for NYCO and model fabrics. Plots of pressure drop across the cloth versus air-flow through the cloth were very similar for NYCO and the model cloths. As a consequence, a comparison of NYCO to model fabrics of known pore size, open area and thickness is a useful method of characterization of NYCO. The air-flow data were modeled in two ways. In the first, a good fit to the data was obtained by applying a model based on air-flow through a single pore to cloth data. In the second, data were successfully analyzed based on a model developed for air-flow through wire meshes.

## RECOMMENDATIONS FOR FUTURE WORK

Factors which could contribute to variability in air-flow data need to be evaluated. These include temperature, relative humidity, nonuniformity of fabric samples, effect of any fabric coating, tortuosity of air path and roughness of fabric surface. The mathematical model suggested by Ishizuka needs to be further evaluated and perhaps modified so that thread diameters and mesh opening sizes of simple military fabrics can be predicted and an "effective" open area for other military fabrics can be determined.

It is important to relate this current work on air-flow to other topics in order to completely characterize fabrics. Recent work has been published concerning hydrostatic pressure resistance of membranes (9). In addition, the wetting and penetration of nylon and polyester filters have

been examined (10,11). It would be useful to correlate this type of information with air-flow data for more complete fabric characterization.

It would be of interest in the future to perform a computer simulation of the air-flow problem. Preliminary efforts at modeling air flow through porous media are in progress (12).

This document reports research undertaken at the US Army Natick Research, Development and Engineering Center and has been assigned No. NATICK/TR-891013 in the series of reports approved for publication.

#### REFERENCES

1. Perry, John H., "Perry's Chemical Engineers Handbook", 4th ed., McGraw-Hill Book Co., 5-59 to 5-62, 1963.
2. "CRC Handbook of Chemistry and Physics", 53rd ed., F31-F33, 1972-73.
3. SPECTRUM Catalogue, p. 156, 1987/88.
4. Personal Communication with Spectrum, 1988.
5. McCarthy, J.H., "Steady Flow Past Non-Uniform Wire Grids", J. Fluid Mech., 19, 491, 1964.
6. Turner, J.T., "A Computational Method for the Flow Through Non-Uniform Gauzes: The General Two-Dimensional Case", J. Fluid Mech., 36, 367, 1969.
7. Elder, J.W., "Steady Flow Through Non-Uniform Gauzes of Arbitrary Shape", J. Fluid Mech., 19, 355, 1959.
8. Ishizuka, M., "Air Flow Resistance of Wire Nettings in Natural Convection", ASME Journal of Fluids Engineering, 109, 389, 1987.
9. Kim, B.S. and Harriott, P., "Critical Entry Pressure for Liquids in Hydrophobic Membranes", J. Colloid Interface Sci., 115, 1, 1987.
10. Kawase, T., Fujii, T. and Minagawa, M., "Repellency of Textile Assemblies, Part I: Apparent Contact Angle of Wax-Coated Monofilament Mesh Screen", Textile Res. J., 58, 185, 1987.
11. Kawase, T., Fujii, T. and Minagawa, M., "Repellency of Textile Assemblies, Part II: Apparent Contact Angle of Fresh Monofilament Mesh Screen", Textile Res. J., 58, 686, 1987.
12. Coulaud, O., Morel, P. and Caltagirone, J.P., "Numerical Modelling of Nonlinear Effects in Laminar Flow Through a Porous Medium", J. Fluid Mech., 190, 393, 1988.

APPENDIX A

Raw Data for Air-flow Measurements

FLOW RATE q (m <sup>3</sup> /s) X 10 <sup>-5</sup>	FLOW RATE Q (m <sup>3</sup> /s/m <sup>2</sup> )	PRESSURE CHANGES IN PASCALS FOR CLOTH SAMPLES							
		*NYCO	*10μm	21μm	33μm	43μm	53μm	67μm	80μm
1.92	0.280	560	430	37	20	12	10	4.5	4.0
2.74	0.400	920	600	57	28.4	17	15	7.0	6.0
3.54	0.517	1200	820	77	38.6	23	21	9.5	8.2
4.38	0.639	1570	1000	95	46.6	28.9	25.6	12	10
5.19	0.758	1930	1300	110	56.5	34.9	31.1	14	12
6.01	0.877	2260	1460	130	66.0	41.3	36.8	17	15
6.84	0.998	2660	1660	150	75.7	47.6	42.8	20	17
7.66	1.12	3060	1930	170	86.6	54.0	49.0	23	20
8.48	1.24	3500	2180	190	97.4	59.8	55.5	25.9	23
9.30	1.36	3920	2430	210	110	69.0	61.5	28.6	25.6
10.13	1.48	4320	2690	230	121	76.2	69.7	32.4	28.9
10.95	1.60	4790	3010	256	135	84.4	77.4	36.4	32.6
11.77	1.72	5320	3350	284	149	94.4	87.2	40.3	36.1
12.60	1.84	5850	3700	306	163	105	95.9	44.3	40.3
13.42	1.96	6380	3990	329	176	113	104	48.6	44.3
14.24	2.08	6920	4390	354	192	122	114	53.3	48.1
15.06	2.20	7450	4720	378	206	134	124	57.5	52.3
15.89	2.32	7980	5050	406	224	144	133	62.0	57.0
16.71	2.44	8650	5450	436	241	156	144	67.2	61.3
17.53	2.56	9240	5850	468	261.9	169	158	73.0	66.7
18.35	2.68	9980	6320	500	280.4	183	170	78.7	72.7
19.18	2.80	10600	6850	533	300.8	196	183	84.7	78.2

\*Pressures obtained with a guage reading up to 100 mm Hg.

## APPENDIX B

### LIST OF SYMBOLS USED

$P_1$	Pressure at upstream pressure tap
$P_2$	Pressure at downstream pressure tap
$\beta$	Ratio of pore to pipe diameter
$g_c$	Dimensional constant
$A$	Cross-sectional area of a pore
$q$	Volume flow rate of air ( $m^3/s$ )
$Q$	Normalized volume flow rate of air ( $m^3/s/m^2$ )
$C$	Discharge coefficient
$Y$	Expansion factor
$C_p$	Specific heat at constant pressure
$C_v$	Specific heat at constant volume
$\delta_p$	Pressure drop across a sample ( $p_1 - p_2$ )
$\rho$	Air density
$K$	Resistance coefficient
$\beta_1$	Porosity (ratio of open area to total area)
$M$	Mach number
$R$	Reynold's number
$\eta$	Fluid (air) viscosity
$d$	Wire (thread) diameter
$s$	Fraction of solid area ( $1 - \beta_1$ )
$w$	Average linear upstream velocity

Distribution List

Names	Copies	Names	Copies
Commander U.S. Army Natick Research, Development and Engineering Center ATTN: STRNC-UE	1	Commander U.S. Army Logistics Center ATTN: ATCL-MS	1
STRNC-UA	1	Fort Lee, VA 23801	
STRNC-IT	1	Director U.S. Army Human Engineering Laboratory	
STRNC-YM	1	ATTN: AMXHE-FS	1
STRNC-YE	1	Aberdeen Proving Ground, MD 21005	
STRNC-YS (J. Halliday)	1	Franklin Institute Research Laboratory	
STRNC-MSR	1	Benjamin Franklin Parkway Philadelphia, PA 19103	1
STRNC-MIL	6	Clemson University School of Textiles 161 Sirrine Hall	
STRNC-AC (M. Lightbody)	1	Clemson, SC 29631	1
Natick, MA 01760-5020		Fabric Research Laboratories Dedham, MA 02026	1
Director U.S. Navy Clothing & Textile Facility ATTN: NCTRF-51	1	Commander U.S. Army Ballistic Research Laboratories	
Natick, MA 01760-5020		Aberdeen Proving Ground, MD 21005	1
DTIC Administrator Defense Technical Information Center Alexandra, VA 22314	1	Commander Air Force Materials Laboratory	
Battelle Edgewood Operations/CBIAC ATTN: Nancy Brletich	1	W.P.A.F.B. Dayton, Ohio 45433	1
2113 Emmerton Park Road		Commander Naval Air Development Center ATTN: WR-4	1
Suite 200		Johnsville, PA 19112	
Edgewood, MD 21040		HRB-Singer, Inc. Science Park P.O. Box 60	
Commander U.S.A. Test and Evaluation Command ATTN: AMSTE-TE-T	1	State College, Pa 16801	1
Aberdeen Proving Ground, MD 21005			
U.S. Marine Corps Liaison Officer U.S.A. Test and Evaluation Command Aberdeen Proving Ground, MD 21005	1		
Director U.S.A. Cold Regions Research and Engineering Laboratory ATTN: CRREL	1		
Hanover, NH 03755			
Commander U.S.A. Combined Arms Center Liaison Office ATTN: ATZL-CAA-L	1		
Ft. Richardson, AK 99505			
Commander U.S. Army Materiel Command Materiel Readiness Support Activity ATTN: AMXMD-ED	1		
Lexington, KY 40511-5101			

